

An efficient finite element analysis model for thermal plate forming in shipbuilding

S.L. Arun Kumar^{1a}, R. Sharma^{*1} and S.K. Bhattacharyya^{2b}

¹*Design and Simulation Laboratory, Department of Ocean Engineering, IIT Madras, Chennai (TN) - 600036, India*

²*Department of Naval Architecture and Offshore Engineering, AMET University, Kanathur (TN) - 603112, India*

(Received October 20, 2023, Revised December 12, 2023, Accepted December 15, 2023)

Abstract. Herein, we present the design and development of an efficient finite element analysis model for thermal plate forming in shipbuilding. Double curvature shells in the ship building industries are primarily formed through the thermal forming technique. Thermal forming involves heating of steel plates using heat sources like oxy-acetylene gas torch, laser, and induction heating, etc. The differential expansion and contraction across the plate thickness cause plastic deformation and bending of plates. Thermal forming is a complex forming technique as the plastic deformation and bending depends on many factors such as peak temperature, heating and cooling rate, depth of heated zone and many other secondary factors. In this work, we develop an efficient finite element analysis model for the thermo-mechanical analysis of thermal forming. Different simulations are reported to study the effect of various parameters affecting the process. Temperature dependent properties are used in the analysis and the finite element analysis model is used to identify the critical flame velocity to avoid recrystallization of plate material. A spring connected plate is modeled for structural analysis using spring elements and that helps in identifying the resultant shapes of various thermal forming patterns. Finally, detailed simulation results are reported to establish the efficacy, applicability and efficiency of the designed and developed finite element analysis model.

Keywords: finite element analysis; flame bending; numerical techniques; ship building; thermal plate forming; transient thermal analysis

1. Introduction

Thermal forming or flame bending is a thermo-mechanical plate forming technique used in the ship building industry for bending plates to obtain complex shapes including double curvature profiles. The driving force for the process is the temperature gradient occurring across the thickness of the plate. This will lead to differences in the expansions occurring across the plate thickness. The resulting temperature gradient and subsequent cooling lead to the plastic deformation and bending of plates.

Although, heating is considered to be a cost effective method, it is a difficult process to control.

*Corresponding author, Ph.D., E-mail: rajivatri@iitm.ac.in

^aResearch Scholar, E-mail: arun.clge@gmail.com

^bProfessor, E-mail: skbhskbh@ametuniv.ac.in

Moreover the curvatures have specific local characteristics as in case of ships (Thomas *et al.* 2018).

When a heat source such as oxy-acetylene flame/laser is made to travel across the plate length, a temperature gradient develops across the plate thickness which is considered to be the principal driving force that enables the bending of plates. Heat affected zone experiences compressive stresses from the adjacent comparatively cooler zone resulting in an initial thermo-elastic bending in the reverse direction. Subsequent cooling of the plate results in a thermo-plastic bending in the opposite direction resulting in a permanent bending angle. Key factors that influence the amount of deformation are: maximum temperature, the heating and cooling rate, and width and depth of the heated zone, etc. Plate dimensions, the heated length, the plate restraint and state of pre-strain in the plate are considered to be secondary factors (Iwamura and Rybicki 1973). As strains and stresses do not affect the temperature profile, thermal forming can be considered as a weakly coupled thermo mechanical process. The involvement of non-linear plastic deformation in a high temperature field that varies with time and space, makes it a complex problem to analyse, (Moshaiov and Vorus 1987).

Some research works exist that report on the optimization of thermal forming technique, e.g. two dimensional beam models and three dimensional plate models have been used by researchers to analyse the process. Iwamura and Rybicki (1973) used a simplified beam model normal to the heating line and a finite difference approach to analyse the process. The total strain which is the sum of elastic, plastic and thermal strains were assumed to be linearly varying in the plate thickness direction. With this assumption and using the equilibrium, continuity and boundary conditions, they developed a set of non-linear simultaneous equations and these were solved using the finite difference technique. The material properties were taken as temperature dependent and the numerical solutions were compared with the experimental results. Moshaiov *et al.* (1987) adopted a three dimensional approach in which a theory for thermo-elastic-plastic bending of plates was developed and solved the governing equation using the boundary element method. The process is treated as an uncoupled problem as the temperature field generated due to the heating was assumed to be unaffected by the stress-strain field. Ueda *et al.* (1994) developed a three dimensional finite element model incorporating large deformations to study the plate behaviour during the induction heating and subsequent cooling and the same was validated using the experimental results. They concluded that the high surface temperature and fast moving heat source lead to angular distortion whereas slow moving heat source leads to shrinkage. Also, they opined that both the welding and thermal forming are the processes having the same root, e.g. welding is a case of thermal forming with high surface temperature and fast moving heat source. Seong *et al.* (2010) reported two geometrical approaches: distance based method and angle based method to solve the inverse problem in the laser forming process. Das & Biswas (2015) studied the effect of various parameters on thermal forming on mild steel using laser beam and reported that the primary factor in achieving good results in laser bending is number of passes followed by sheet thickness, laser power, and traverse speed, etc.

1.1 Motivation

As flame bending is a complex process owing to its material non-linearity and spatial and time dependent temperature distribution, we believe that the numerical simulations based upon 'Finite Element Analysis (FEA)', ideally suits the objective to avoid the cost and time involved in the experiments. Hence, we focus on the design and development of an efficient finite element analysis model for thermal plate forming in shipbuilding and investigate the various aspects of it, in-detail. During the structural analysis with FEA, in order to avoid the rigid body motion, the nodes need to

be fixed and this leads to the requirement of changing the structural boundary conditions for different heating patterns in order to obtain meaningful solutions for the problem. *We address this problem in the present work and model the plate using spring elements that can be used for solving problems irrespective of the heating patterns.* Resultant shapes of the plates subjected to various heating patterns are obtained using the spring connected model through FEA and detailed numerical simulations are performed to identify the effect of various factors involved in the thermal forming. *We can note here that since in the shipbuilding plates are thermally formed while they rest (or are simply supported) over a bed/support consisting of flattened/rounded spokes, our idea of using the spring support condition represents the real world in close approximation.* Additionally, in comparison with other type of boundary conditions where the displacements/rotations at the surface of contact are fixed, the spring boundary condition allows the surface to move during the analysis which in turn creates reaction forces acting on the structure at the boundary surface.

1.2 Objective and scope

Primarily, our objective is to design, develop and implement an effective FEA based numerical simulation model for thermal forming and we aim for:

- To identify the effect of various parameters in thermal forming for thick plates.
- To determine the critical flame velocities to avoid recrystallization of plate material during thermal forming.
- To develop a spring connected model that can predict the resulting shape of the plate subjected to different types of heating patterns.

2. Finite element analysis based model for plate bending

The FEA requires systematic considerations to determine the influence of specific factors such as creep, hardening, yield point variation with temperature and Young's modulus variation with temperature on the constitutive relations, (Moshaiov & Vorus, 1987). Herein, we consider the temperature dependency of yield point and Young's modulus. However the effect of creep is neglected as the plate experiences high temperatures for relatively only a short time period. Temperature field is assumed to be unaffected by the structural response and hence the thermal and structural problems are solved sequentially. Results from the transient thermal analysis is used as input for the structural analysis. Complete methodology for the FEA based thermo-mechanical analysis of plate bending process is shown in Fig. 1.

2.1 Governing equation for transient thermal analysis

Following Lewis *et al.* (1996), Bergman *et al.* (2011), and Biswas *et al.* (2011), the governing equation for heat conduction is

$$\frac{\partial}{\partial x} \left(k \frac{\partial T}{\partial x} \right) + \frac{\partial}{\partial y} \left(k \frac{\partial T}{\partial y} \right) + \frac{\partial}{\partial z} \left(k \frac{\partial T}{\partial z} \right) = \rho c \frac{\partial T}{\partial t} \quad (1a)$$

where the temperature (T) is a function of space coordinates (x , y and z) and time (t) and the thermal conductivity of plate material (k) depends on the temperature at a particular plate position

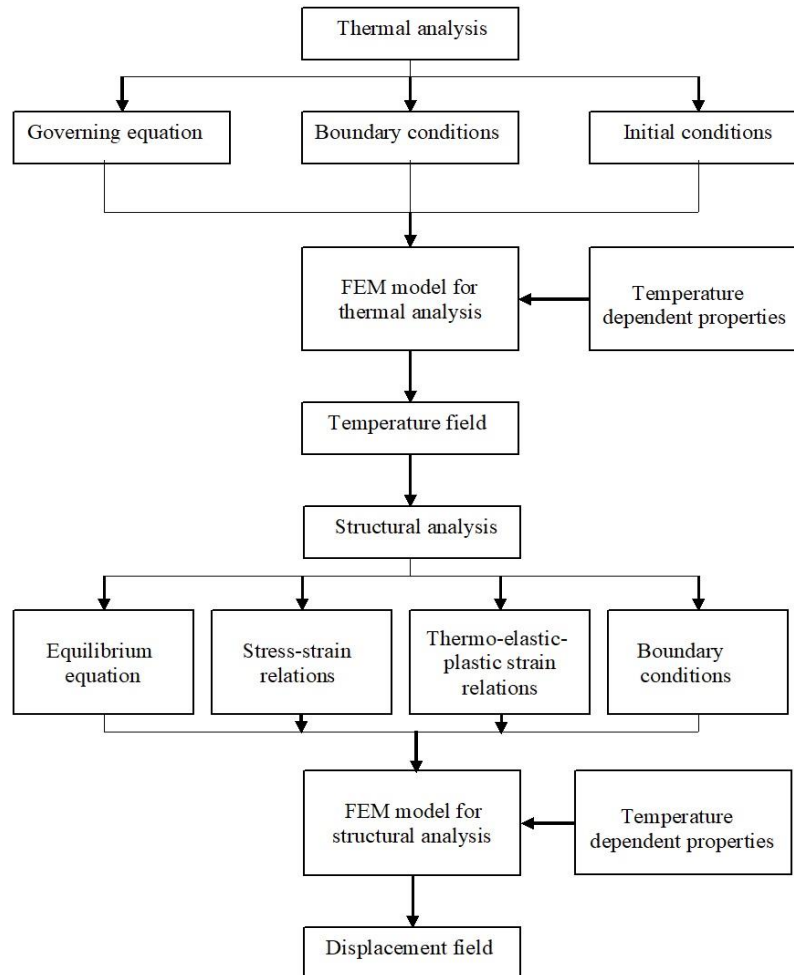


Fig. 1 Methodology for the FEA based thermo-mechanical analysis of plate bending

and ρ and c are the density and specific heat values respectively, and these are also considered as temperature dependent properties for a particular plate material. The convection heat transfer from the plate is modelled using Newton's law of cooling (Biswas *et al.* 2011), and is defined as

$$q_{conv} = h_f(T - T_\infty) \quad (1b)$$

where q_{conv} represents the convection heat loss from the surface of the plate at temperature T . Here, h_f denotes the heat transfer coefficient, a temperature dependent property for a particular plate material, while T_∞ represents the ambient temperature.

We consider the mild steel as the plate material for transient thermal analyses and elasto-plastic analyses, and the temperature dependencies of thermal conductivity, specific heat and heat transfer coefficient are shown in Figs. 2 (a)-2(c), respectively, adapted from Biswas *et al.* (2011). We note here that the heat transfer via radiation mode is not considered in our present work, as it is assumed to be negligible when compared with the other two modes of heat transfer.

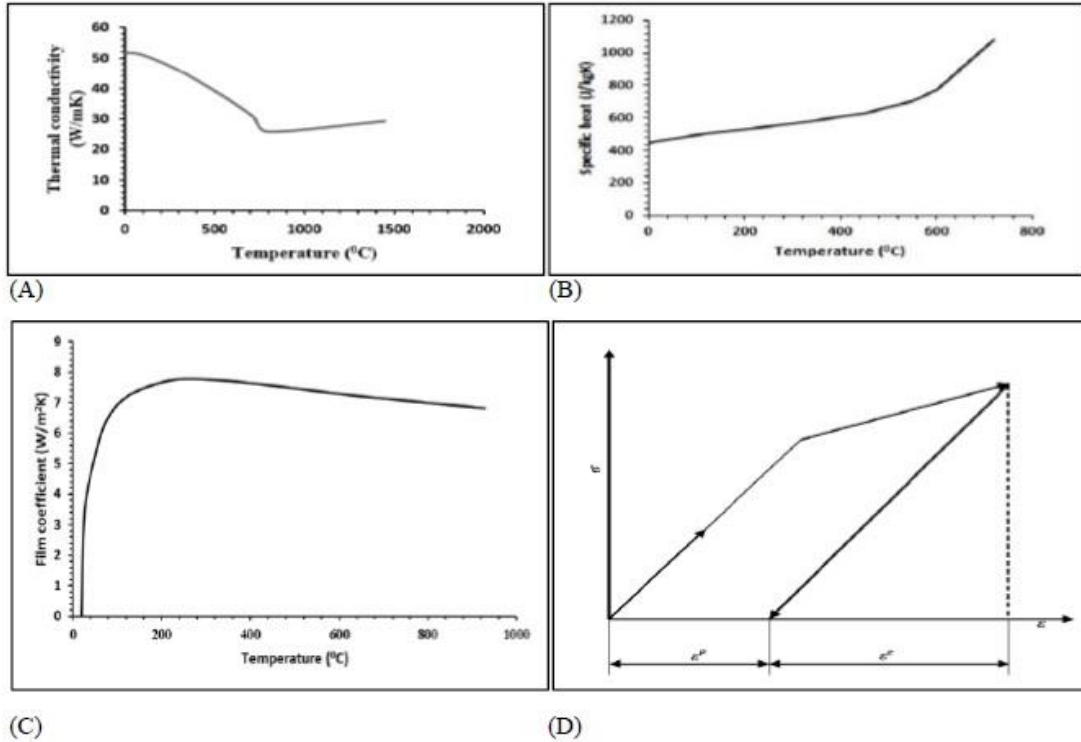


Fig. 2 (a) Variation of thermal conductivity with temperature; (b) Variation of specific heat with temperature; (c) Variation of film coefficient with temperature; and (d) One dimensional plastic behaviour

2.2 Modelling of heat source

Heat sources should be properly modelled as these are the driving forces for the process (Clausen, 2000). Mathematical models of oxy-acetylene gas torch and laser beams are used in the present work and both of these types of heat sources are modelled using axisymmetric heat flux with Gaussian distribution. Following Clausen (2000), the oxy-acetylene gas torch is modelled

$$Q_p = Q_{max}e^{-\gamma r^2} \tag{2}$$

Through Eq. (2), we note that the point wise heat flux applied at points away from the centre in case of oxy-acetylene flame (Q_p) is considered as a function of maximum value of the distributed heat flux (Q_{max}), width factor γ and distance from the torch centre (r). Total heat input from gas torch to plate (Q_{total}) is modelled (adapted from Biswas *et al.* (2011))

$$Q_{total} = \int_0^{2\pi} \int_0^{\infty} Q_p r dr d\theta = \frac{\pi Q_{max}}{\gamma}; \gamma = \frac{\ln 100}{r_{torch}^2} \tag{3}$$

where r_{torch} is the radius of the oxy-acetylene flame and that is taken as 4 cm in this work unless otherwise specified. Following Zhang *et al.* (2004), the mathematical model for the heat flux distribution (q'_p) from the laser beam is

$$q'_p = \frac{3\eta Q'}{\pi R^2} [e^{-3((\frac{x}{R})^2 + (\frac{z}{R})^2)}] \quad (4)$$

where η is the laser absorption efficiency, Q' is the input power, R is the radius of the laser at which the amplitude is $\frac{1}{e^3}$ of its center value, and x and z denote the distance of a point as measured from the central point of the laser beam. The laser absorption efficiency is taken as 0.65 in the present work.

2.3 Governing equations for structural analysis

The temperature distribution obtained from thermal analysis is used in the structural analysis to estimate the plastic deformations and bending angles generated in the plate. The plate material expands or contracts and hence is subjected to thermal strains when the plate temperature is raised or lowered respectively. This expansion and contraction of plate material is directly proportional to the change in temperature. A free plate made of homogenous isotropic material experiences no thermal stresses even though there may be thermal strains. The plate subjected to heating experiences thermal stresses because of different conditions and reasons, e.g.:

1. When the temperature distribution is not uniform.
2. Due to restrictions on plate boundaries.
3. Due to the anisotropic and non-homogenous behavior of the plate material as in case of bimetallic plates.

Following Ugural (2010), Biswas *et al.* (2007) and Srinath (2009), the equilibrium equations, the constitutive relations and the strain displacement relations and compatibility equations are

$$\begin{aligned} \frac{\partial \sigma_x}{\partial x} + \frac{\partial \tau_{xy}}{\partial y} + \frac{\partial \tau_{xz}}{\partial z} + F_x &= 0 \\ \frac{\partial \sigma_y}{\partial y} + \frac{\partial \tau_{xy}}{\partial x} + \frac{\partial \tau_{yz}}{\partial z} + F_y &= 0 \\ \frac{\partial \sigma_z}{\partial z} + \frac{\partial \tau_{xz}}{\partial x} + \frac{\partial \tau_{yz}}{\partial y} + F_z &= 0 \end{aligned} \quad (5)$$

$$\{\sigma\} = [D]\{\varepsilon\} \quad (6)$$

$$\varepsilon_x = \frac{\partial u}{\partial x}; \quad \varepsilon_y = \frac{\partial v}{\partial y}; \quad \varepsilon_z = \frac{\partial w}{\partial z},$$

$$\gamma_{xy} = \frac{\partial u}{\partial y} + \frac{\partial v}{\partial x}; \quad \gamma_{yz} = \frac{\partial v}{\partial z} + \frac{\partial w}{\partial y},$$

$$\gamma_{xz} = \frac{\partial u}{\partial z} + \frac{\partial w}{\partial x}; \quad \frac{\partial^2 \varepsilon_x}{\partial y^2} + \frac{\partial^2 \varepsilon_y}{\partial x^2} = \frac{\partial^2 \gamma_{xy}}{\partial x \partial y},$$

$$\frac{\partial^2 \varepsilon_y}{\partial z^2} + \frac{\partial^2 \varepsilon_z}{\partial y^2} = \frac{\partial^2 \gamma_{yz}}{\partial y \partial z}; \quad \frac{\partial^2 \varepsilon_z}{\partial x^2} + \frac{\partial^2 \varepsilon_x}{\partial z^2} = \frac{\partial^2 \gamma_{xz}}{\partial x \partial z},$$

$$\frac{\partial}{\partial z} \left(\frac{\partial \gamma_{yz}}{\partial x} + \frac{\partial \gamma_{zx}}{\partial y} - \frac{\partial \gamma_{xy}}{\partial z} \right) = 2 \frac{\partial^2 \varepsilon_z}{\partial x \partial y}; \quad \frac{\partial}{\partial x} \left(\frac{\partial \gamma_{zx}}{\partial y} + \frac{\partial \gamma_{xy}}{\partial z} - \frac{\partial \gamma_{yz}}{\partial x} \right) = 2 \frac{\partial^2 \varepsilon_x}{\partial y \partial z},$$

$$\text{and } \frac{\partial}{\partial y} \left(\frac{\partial \gamma_{xy}}{\partial z} + \frac{\partial \gamma_{yz}}{\partial x} - \frac{\partial \gamma_{zx}}{\partial y} \right) = 2 \frac{\partial^2 \varepsilon_y}{\partial x \partial z} \quad (7)$$

where $\sigma_x, \sigma_y, \sigma_z$ are the normal stresses in the x, y and z planes respectively; $\tau_{xy}, \tau_{yz}, \tau_{zx}$ are the shear stresses in the x, y and z planes respectively and parallel to y, z and x directions; F_x, F_y, F_z are the x, y and z components of body forces per unit volume; $\{\sigma\}$ is the stress vector; $[D]$ is the stiffness matrix; $\{\varepsilon\}$ is the strain vector; $\gamma_{xy}, \gamma_{yz}, \gamma_{zx}$ are the shear strains in the x-y, y-z and x-z planes and u, v, w are the displacements in the x, y and z directions respectively. These Equations (5-7) along with structural boundary conditions are used to determine the strains and displacement field which in turn is used for determining the extend of bending. Following, Moshaiov and Vorus (1987), the thermal (ε^{th})-elasto (ε^e)-plastic (ε^p) strain relationship is

$$\varepsilon = \varepsilon^e + \varepsilon^p + \varepsilon^{th} \quad (8)$$

The ε is known as additive decomposition of strains applicable for small strains and it is the superposition of the increment of elastic, plastic and thermal strains. Fig. 2 (d) shows the one dimensional plastic behavior, adapted from Moshaiov and Vorus (1987). Following Biswas *et al.* (2011), the Young's modulus of elasticity (E), Poisson's ratio (μ), coefficient of thermal expansion and yield stress of the plate material are assumed to be temperature dependent and their variations with reference to temperature are shown in Figs. 3(a)-3(d).

2.4 Modelling plasticity

Our study involves analyzing the deformation (or bending) of plates through thermal forming using numerical techniques which involves plastic deformation. The theory of plasticity establishes the relationship that characterizes elasto-plastic response of the material when it is subjected to strains in the elasto-plastic regime. Modelling of plasticity involves three elements: Yield criterion, flow rule and hardening rule. Following Ansys (2009), the yield criterion, flow and hardening rules are

$$\sigma_e = f(\{\sigma\}) \quad (9)$$

where $\{\sigma\}$ is the stress vector and σ_e is the equivalent stress. The material will develop plastic strains, when the equivalent stress equals the material's yield value.

In case of multi-axial stress system, von Mises is the well-known criterion usually adopted, and the yield surface of which is elliptical in nature. The region inside the yield surface depicts the elastic regime and any stress state on the yield surface depicts elasto-plastic regime. Again, following Ansys (2009), the material flow beyond the initial yield point is defined by

$$\{d\varepsilon^p\} = \lambda \left\{ \frac{\partial Q}{\partial \sigma} \right\} \quad (10)$$

where λ is the plastic multiplier and Q is the plastic potential which is a function of stress. Isotropic hardening that involves uniform yield surface expansion with plastic strain is utilized in this work and the hardening rule is

$$F(\{\sigma\}, \kappa, \{\alpha\}) = 0 \quad (11)$$

where κ is the plastic work and $\{\alpha\}$ is the translation of yield surface.

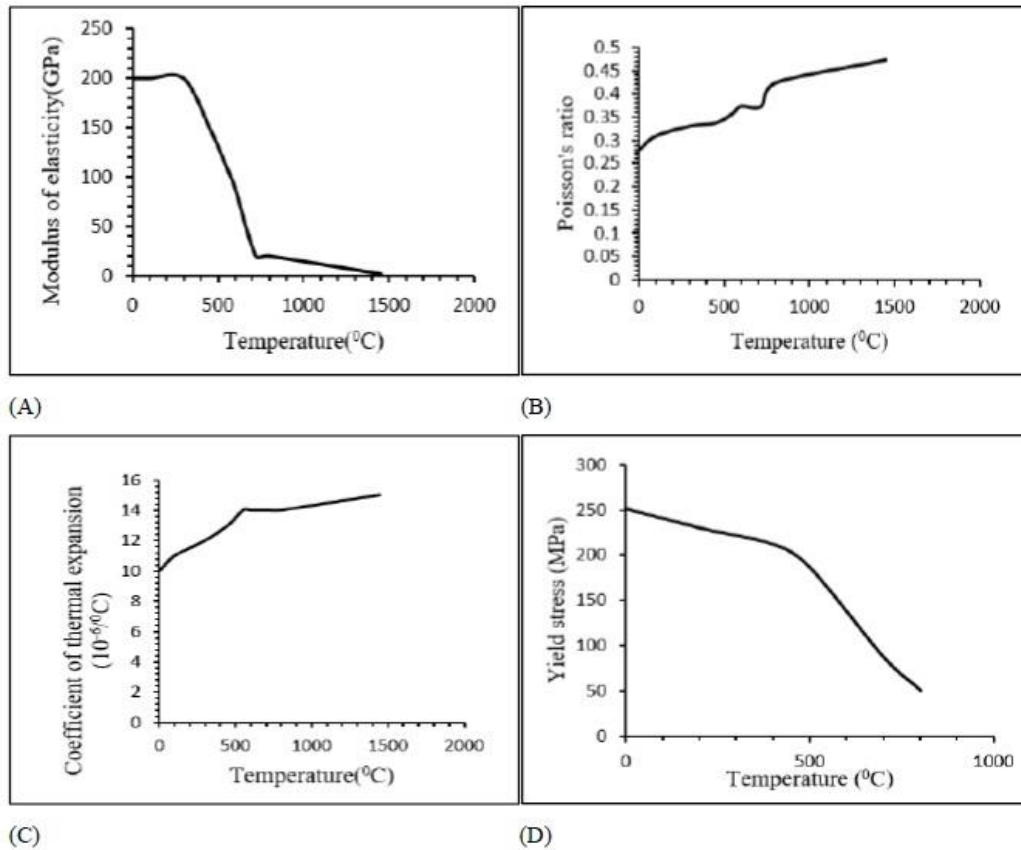


Fig. 3 (a) Variation of the Young's modulus of elasticity with temperature, (b) Variation of the Poisson's ratio with temperature, (c) Variation of the coefficient of thermal expansion with temperature; and (d) Variation of yield stress with temperature

2.5 Finite element 3-D geometric model

Numerical model present in the present work is implemented in the AnsysTM mechanical APDL software solution system and a rectangular plate with required dimensions is modelled using different element types as available in the AnsysTM elements' library. The mesh details for thermal and structural analyses are:

- *Thermal analysis:* In case where the objective is to determine the temperature distribution and related analyses, variable meshing with finer meshes in the central region and coarser meshes away from the centre as shown in Fig. 4(a), is used. A total of 13481 eight noded brick elements are used beyond which not much variations have been observed.

- *Structural analysis:* Two steps are involved in determining the displacement values. In the first step, a thermal analysis is done using eight noded thermal brick element and in the second step, the temperature field obtained from the first step is used in structural analysis to determine the inherent displacements using eight noded structural brick element. Both the analyses are done using a plate model uniformly meshed (Fig. 4(b)) with 30000 elements beyond which not much variation has

been found. Furthermore, spring element is used to estimate the final deformations of the plates supported by springs. Overall, the idea is to develop and implement a FE model as shown in Fig. 4 (C) that can predict the resulting shape of the plate subjected to different types of heating patterns.

3. Thermal analyses for thermal forming using a validated FEA model

As noted before, our numerical model present is implemented in the AnsysTM mechanical APDL software solution system and we determinine the temperature distribution in the plate subjected to thermal forming. We start with a process of verification and validation and for this we benchmark/compare our simulation results with these of Zhang *et al.* (2004). Figs. 4(d) and 5(a) show the comparison of our numerical results (Tsimu) with the experimental results (Texp) of Zhang *et al.* (2004). In their work, a laser beam of radius 7 mm was used as the heat source with a torch speed of 9.5 mm/s and heat input of 2700 W. The thermal forming was performed on a 304.8x304.8x19.05 mm rectangular plate. We model the laser heat flux distribution as the Gaussian distribution as discussed previously in Section 2.2. In our implementation, following Biswas *et al.* (2007), the boundary conditions are

$$\begin{aligned} & \text{- At time, } t = 0, \text{ temperature, } T = T_{\infty}, \text{ where } T_{\infty} \\ & \text{is the initial temperature which is same as the ambient temperature.} \end{aligned} \quad (12)$$

$$\text{- At } t > 0, q_n = -q_{sup}, \text{ along the heating region.}$$

Here, q_n is the normal component of the conduction heat flux vector with respect to the plate surface and q_{sup} is the heat flux supplied by the heat source. (13)

$$\text{- At } t > 0, q_n = h_f(T - T_{\infty}), \text{ for regions away from the heating line.} \quad (14)$$

Figs. 5(b) and 5(c) show the comparison of our numerical results with experimental results of Biswas *et al.* (2007). In their work, a 40 mm radius oxy-acetylene flame was used to heat 300x260 mm mild steel plates of 6 and 8 mm thicknesses. Heat input was taken as 5350 W and the flame velocity was 0.36 m/min. The heat flux distribution from oxy-acetylene flame is modelled as Gaussian distribution as discussed previously in section Section 2.2 and the discretised geometrical model with variable meshes are used for numerical code's verification and validation purposes, as reported here. As a summary of the verification and validation studies through extensive comparison of results with those of Zhang *et al.* (2004) and Biswas *et al.* (2007), we can state that as the results and comparisons agree favourably, our numerical model is verified and validated.

3.1 Effect of various parameters on maximum temperature developed

We conducted different numerical simulations to study the effect of heat input, flame characteristics such as flame velocity and flame radius and the plate thickness on the peak temperature developed on plate surface using the designed and developed FEA model reported, verified and validated, as described herein in Section 2 and 3. The results of these simulations are shown in Figs. 5(d), 6(a), 6(b) and 6(c). We also study the effect of heat input to flame velocity on the maximum temperature developed through these simulations and the result is presented in Fig. 6(d).

A 304.8 x 304.8 mm plate with thickness of 19.05 mm is used for the analyses. The maximum temperature developed at the Bottom surface Central Point (BCP) is used/reported for the analyses.

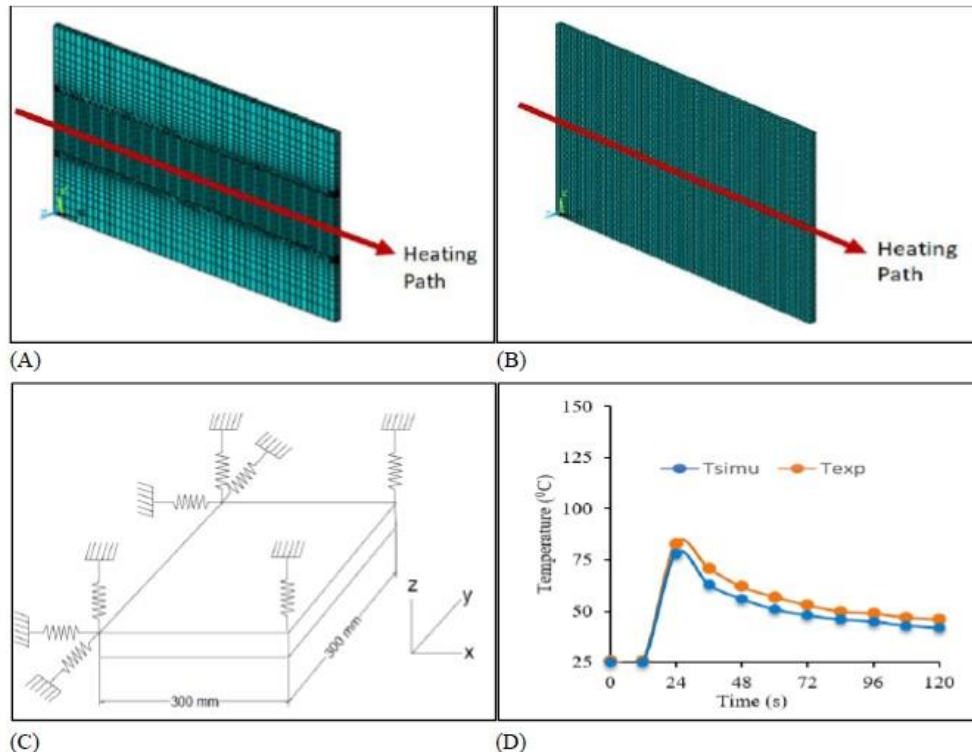


Fig. 4 (a) FEA model with variable meshing, (b) FEA model with uniform meshing, (c) Plate supported by the springs; and (d) Time-Temperature curve at bottom centre of the plate

From these results of Figs. 5(d), 6(a), 6(b) and 6(c), we observe:

- A linear relationship exists between heat input and maximum temperature developed and this is as expected as the temperature increases with increase in heat input.
- We can note that the peak temperature increases with flame radius initially. However beyond a certain flame radius value, it is observed that the peak temperature is not much affected by the increase in flame radius.
- As the flame velocity increases, the contact time between the plate surface and flame decreases leading to less penetration of heat in to the plate and hence the peak temperature developed at higher flame velocity is comparatively lower than that developed at lower flame velocity.
- The peak temperature developed in a plate subjected to thermal forming decreases with increase in plate thickness. The increase in plate thickness increases the volume/cross sectional area of the plate and in turn increases the convection heat transfer rate leading to the drop in peak temperature.
- The ratio between heat input and flame velocity is found to affect the maximum temperature developed during flame bending. Higher the Q/v ratio, higher will be the peak temperature developed.

3.2 Time-temperature history analysis across the plate thickness

Using Figs 7(a)-7(c), we show and analyze the time-temperature history of central points of opposite surfaces of 6 mm, 50 mm and 100 mm thick plates obtained through FEA model's

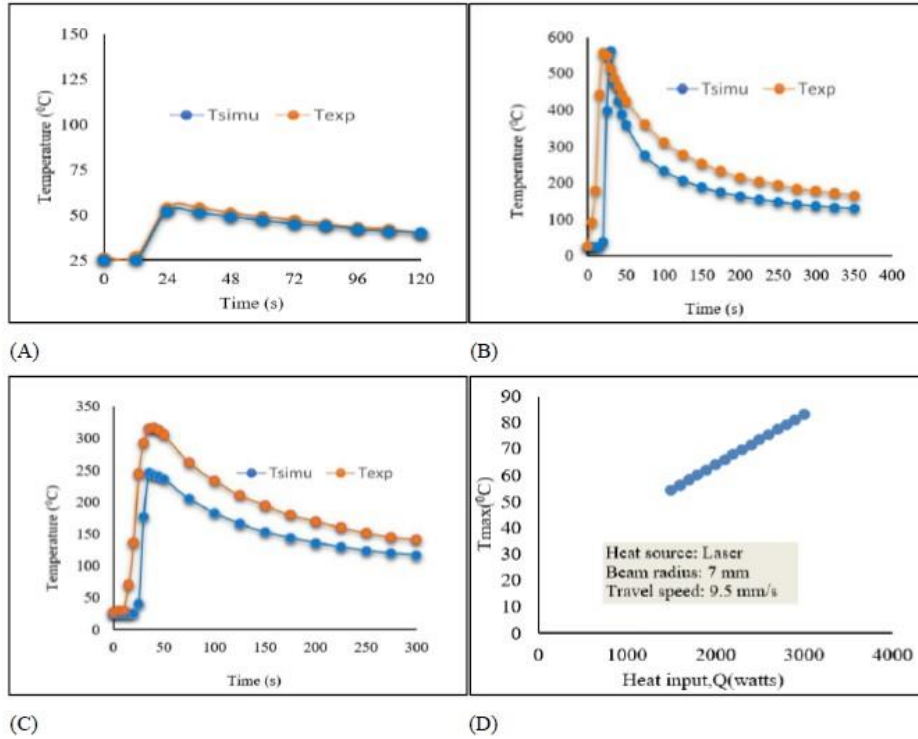


Fig. 5 (a) Time-Temperature curve at the location of 20 mm away from top centre of the plate, (b) Time-Temperature curve on top surface of 6 mm thick plate, (c) Time-Temperature curve on top surface of 8 mm thick plate at the location of 20 mm away from heating line; and (d) Effect of heat input on maximum temperature developed

numerical simulations. The flame travel is as shown in Fig. 7(d). Here ‘A’ is the ‘Top-surface Central Point (TCP)’ located at the central point of the plate surface on which flame is moving and ‘B’ is the corresponding ‘Bottom-surface Central Point (BCP)’ located on the surface opposite to that subjected to thermal forming. From these analyses, we observe that the top surface temperature significantly affects temperature distribution of the bottom surface for thin plates and for thicker plates the influence is ‘negligible’. A large number of FEA numerical simulations are performed for plate thicknesses above 12 mm for studying the variation in the difference in the peak temperatures developed at the top and bottom surfaces of the plate (ΔT_p) and it is defined:

$$\Delta T_p = TCP - BCP \tag{15}$$

Results are shown in Fig. 8(a). Different adopted numerical parameters used in the FEA numerical simulations are listed in Table 1.

3.3 The effect of flame velocity on temperature profiles

We study the effect of flame velocity in the temperature profiles, through numerical simulations, using the parameters listed in Table 2 and the flame travel path is as shown in Fig. 7(d). Resulting time-temperature profiles are shown in Figs. 8(b)-8(d).

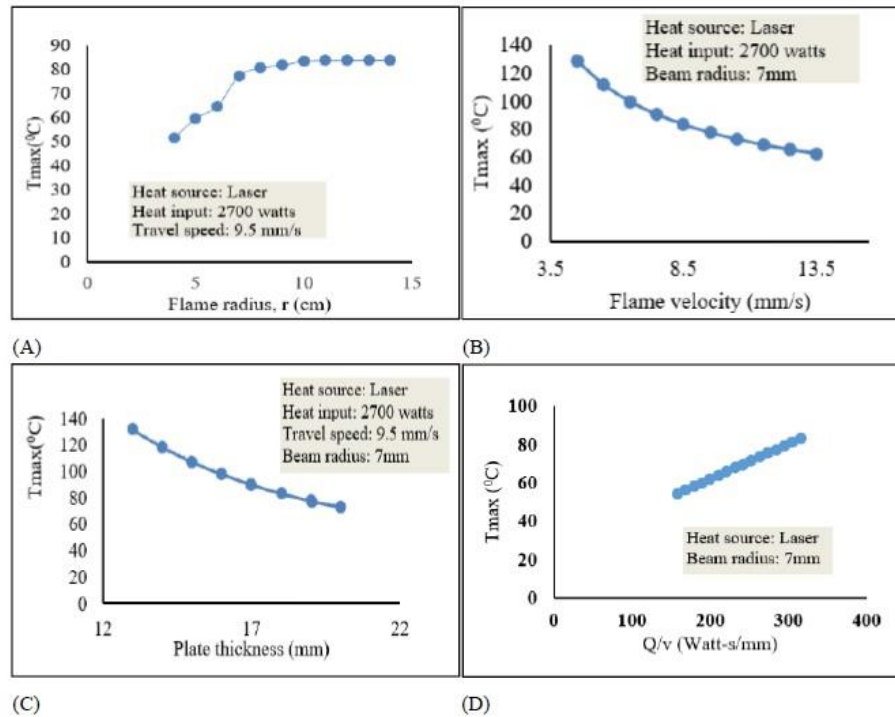


Fig. 6 (a) Effect of flame radius (in mm) on maximum temperature (in $^{\circ}\text{C}$), (b) Effect of flame velocity (in mm/s) on maximum temperature (in $^{\circ}\text{C}$) developed, (c) Effect of plate thickness (in mm) on maximum temperature (in $^{\circ}\text{C}$) developed; and (d) Effect of Q/v (in m-s/mm) on maximum temperature (in $^{\circ}\text{C}$) developed

Table 1 Different adopted numerical parameters used in the FEA numerical simulations

| Heat input | Flame type | Flame radius | Flame velocity | Plate dimension |
|------------|---------------|--------------|----------------|-----------------|
| 6350 watts | Oxy-acetylene | 4 cm | 6 mm/s | 300 mm x 300 mm |

Table 2 Numerical parameters for studying the effect of flame velocity

| Heat input | Flame type | Flame radius | Plate dimension |
|------------|---------------|--------------|------------------------|
| 6350 watts | Oxy-acetylene | 4 cm | 300 mm x 300 mm x 6 mm |

Ratio of peak BCP temperature to peak TCP temperature ($T_p(\text{BCP})/T_p(\text{TCP})$) decreases with increase in flame velocity as shown in Fig. 9(a).

3.4 Critical flame velocity to avoid recrystallization of plate material

We make an attempt to determine the velocity of the flame below which the temperature of the plate material may rise above its recrystallization temperature for various plate thicknesses using the FEA model developed. Herein, the recrystallization temperature is taken as 650°C (Moshaiov and Vorus 1987). Flame velocity below which the peak temperature of the plate material may cross

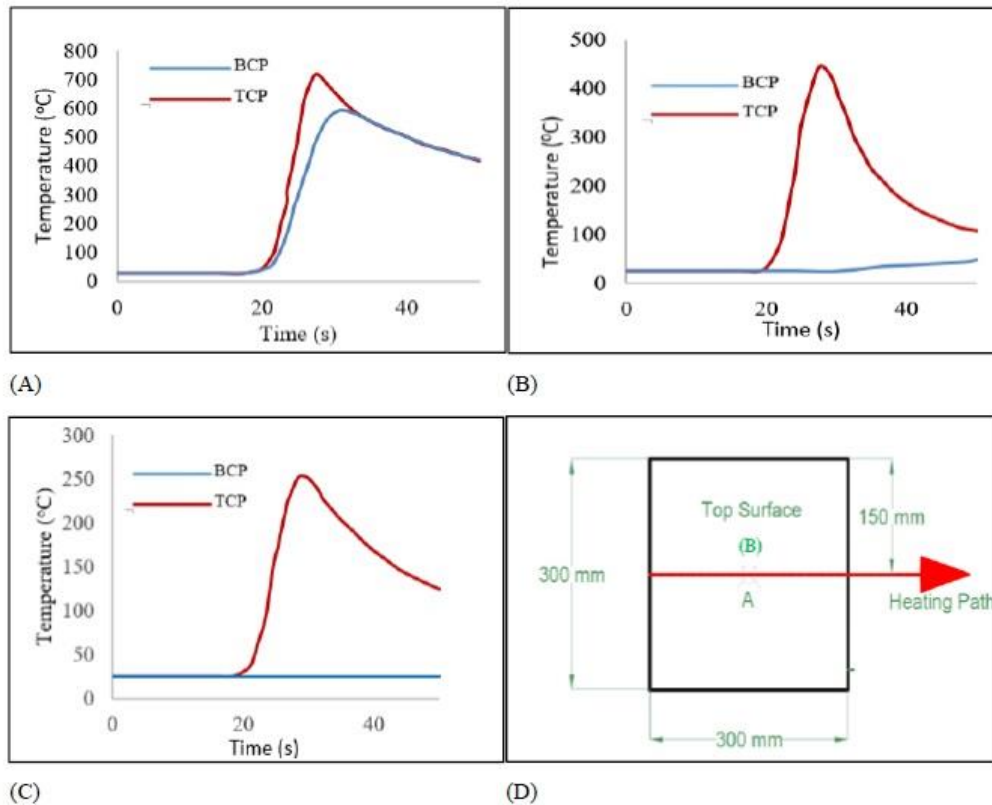


Fig. 7 (a) Time-Temperature history for 6 mm thick plate, (b) Time-Temperature history for 50 mm thick plate, (c) Time-Temperature history for 100 mm thick plate; and (d) Line heating pattern for numerical analysis

its recrystallization temperature is termed here as '*critical flame velocity*'. Several numerical simulations with numerical parameters as listed in Table 3 are performed towards this goal and the peak temperature observed at the midpoint on the top surface of the plate (point A as shown in Fig. 7(d)) is used to find the relation. Fig. 9(b) shows the variation of critical velocity with plate thicknesses and we observe that the critical velocity decreases with increase in plate thickness.

3.5 Time-Temperature history analysis of plates subjected to top and bottom surface thermal forming

Heating the plate on the top surface will raise the temperature of the bottom surface and vice-versa, particularly in thin plates. Numerical simulations are performed to analyze the time-temperature curves obtained for the plate subjected to thermal forming and these are based on the numerical parameters given in Table 3. At first, the plate is heated on top surface and during the second pass, the bottom surface is heated as shown in Fig. 7(d). Figs. 9(c), 9(d) and 10(a) show the time-temperature curves of the top and bottom surface central points for the plates subjected to double pass thermal forming as per the heating pattern described in Fig. 7(d). Flame velocity is taken as 6 mm/s. The red and blue curves indicate the temperature – time history of points A and B

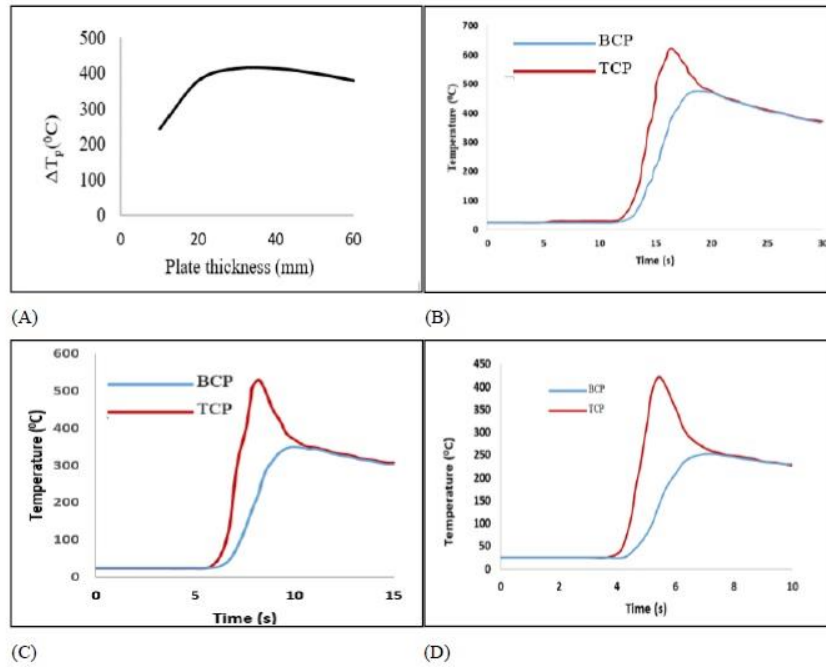


Fig. 8 (a) Variation of ΔT_p with plate thickness, (b) Time-Temperature profile for 10 mm/s flame velocity; (c) Time-Temperature profile for 20 mm/s flame velocity; and (d) Time-Temperature profile for 30 mm/s flame velocity

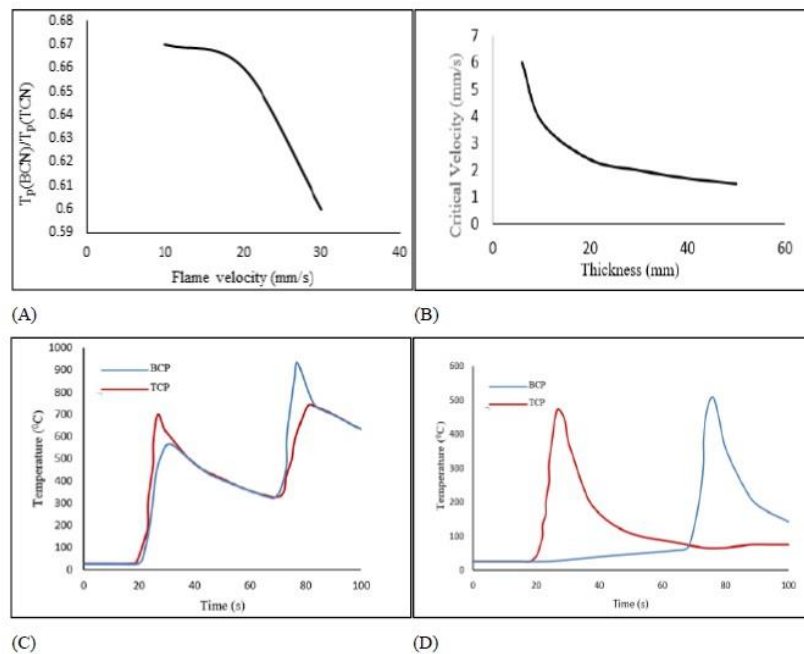


Fig. 9 (a) Variation of the $T_p(BCP)/T_p(TCP)$ versus flame velocity, (b) Variation of critical flame velocity with plate thickness, (c) Time-temperature history for 6 mm thick plate subjected to double pass thermal forming; and (d) Time-temperature history for 50 mm thick plate subjected to double pass thermal forming

Table 3 Numerical parameters for determining critical flame velocity

| Heat input | Flame type | Flame radius | Plate dimension |
|------------|---------------|--------------|-----------------|
| 6350 watts | Oxy-acetylene | 4 cm | 300 mm x 300 mm |

Table 4 Numerical Thermal forming parameters for structural analysis

| Heat input | Flame type | Flame radius | Flame velocity | Plate dimension |
|------------|---------------|--------------|----------------|------------------------|
| 6350 watts | Oxy-acetylene | 4 cm | 0.36 m/minute | 300 mm x 260 mm x 6 mm |

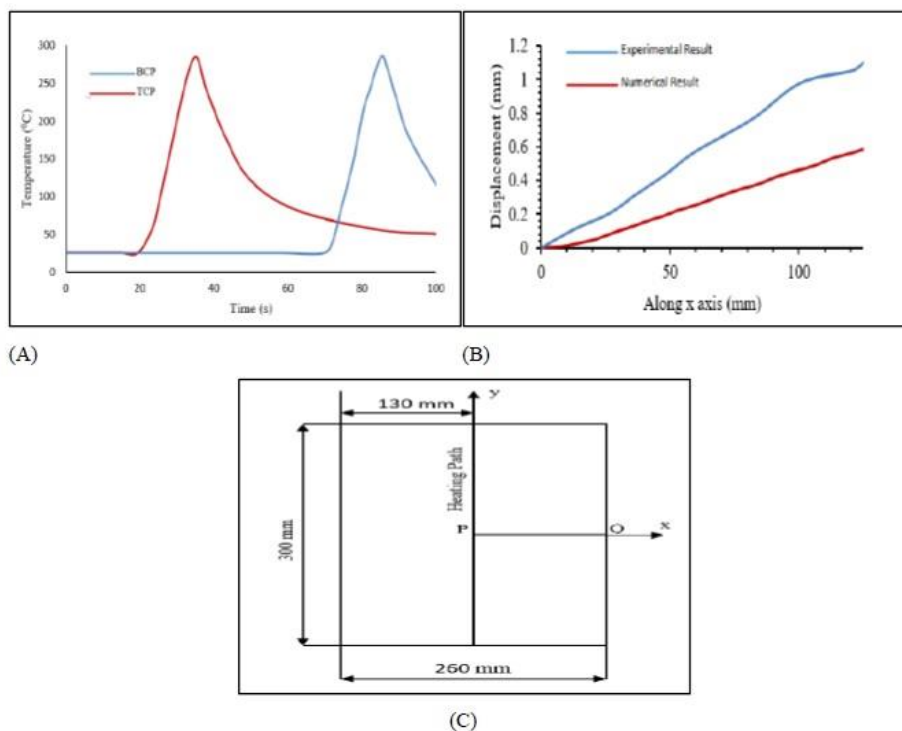




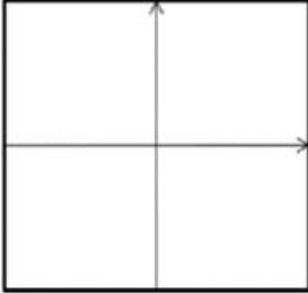

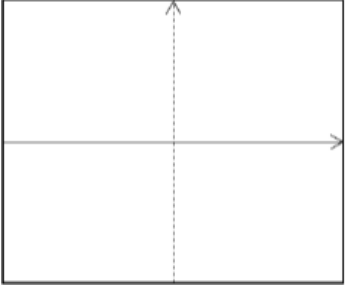
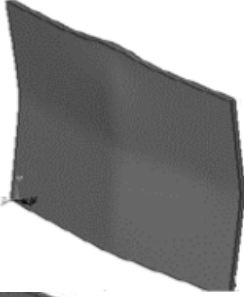
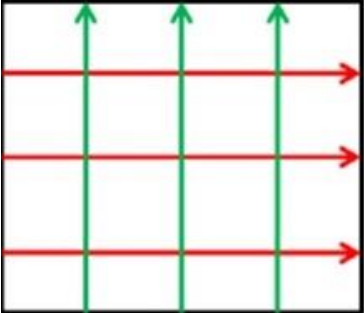

Fig. 10 (a) Time-temperature history for 100 mm thick plate subjected to double pass thermal forming, (b) Displacement measured along x axis; and (c) Heating pattern for structural analysis

respectively and we can see that heating one face affects the opposite face considerably for low thickness plates. However as the thickness of the plate increases, heating one face does not significantly raise the temperature of the opposite face.

4. Prediction of final shape using spring connected model

Structural analysis is done on a spring connected plate using the FEA model described herein and the values of the temperature field variables obtained from thermal analysis are used in the FEA model developed for structural analysis to estimate the displacements. Initially the thermal analysis

Table 5 Heating patterns and the resulting deformed shapes

| Heating path | Deformed shape |
|---|--|
|  |  |
|  |  |
|  |  |
|  |  |

is done using a spring connected plate model to determine the temperature distribution and the resulting temperature field is used in performing the elasto-plastic structural analysis to determine the resultant plastic deformation. The 30000 eight-node brick elements with uniform meshing are used for both thermal and structural analysis and the spring elements are fixed to the plate as shown in Fig. 4(c).

Numerical results obtained using the parameters given in Table 4 are compared with experimental results of the work done by Biswas *et al.* in 2007 and the comparison is shown in Fig. 10(b). Here the displacement is measured along the line PQ as shown in Fig. 10(c).

As noted before, 30000 eight-node brick elements with uniform meshing are used for both thermal and structural analysis. The spring elements are fixed to the plate as shown in Fig. 4(c). The numerical results obtained using the parameters given in Table 4 are compared with experimental results of the work done by Biswas *et al.* in 2007 and the comparison is shown in Fig. 10(b). Here the displacement is measured along the line PQ as shown in Fig. 10(c).

The model of plate attached with springs is used in numerical simulations for estimating the final shapes of the plates subjected to thermal forming.

Table 5 shows the heating pattern and corresponding final shape of the deformed plate obtained through numerical simulations. The dotted arrow indicates back surface heating.

5. Conclusions

Finally, from the presented works herein, we can conclude:

- A FEA model has been designed and developed for thermal analysis of thermal forming in plates.
- The peak temperatures that develop in the plate subjected to thermal forming increase with heat input and decrease with flame velocity and plate thickness. However, the peak temperatures developed initially rise with flame radius and reach a maximum level beyond which not much variation has been found.
- We observed that the influence of rise in temperature on the surface of the plate subjected to thermal forming on the opposite surface decreases with increase in plate thickness for a given set of heating conditions.
- With the increase in flame velocity, the ratio of the peak BCP temperature to peak TCP temperature decreases drastically beyond a certain flame velocity when the heating conditions are kept unchanged.
- An attempt has been made to study the variations in critical flame velocity with changes in plate thickness.
- Numerical simulations have been performed to analyze the nature of temperature profiles when the opposite surfaces of the plates are subjected to thermal forming.
- A spring connected FEA model has been developed for predicting the final deformed shapes of the plate subjected to various thermal forming patterns.
- However, herein we have not studied the effect of multiple passes, that requires cooling, to achieve higher bending/curvature. Our future work shall go in these directions and some of these are currently under investigation.

Acknowledgements

This research was supported by the internal research grants of IIT Madras, Chennai, India and the first author was supported by the MoE, GoI, India scholarship scheme (reference number: OE15D019) in the past.

Trademark and copyrights

*Trademark and copyright with the Ansys, Inc., USA, 2023.

References

- Ansys (2009), *Theory Reference for the Mechanical APDL and Mechanical Applications*. 3304 (April), 724-746.
- Bergman, T.L., Lavine, A.S., Incopera, F.P. and Dewitt, D.P. (2011), *Fundamentals of Heat and Mass Transfer*. 7th ed, Hoboken, NJ: Wiley.
- Biswas, P., Mandal, N.R. and Sha, O.P. (2007), “Three-dimensional finite element prediction of transient thermal history and residual deformation due to line heating”, *Proceedings of the Institution of Mechanical Engineers Part M: J. Engineering for the Maritime Environment*, **221**(1), 17-30. <https://doi.org/10.1243/14750902JEME60>.
- Biswas, P., Mandal, N.R., Sha, O.P. and Mahapatra, M.M. (2011), “Thermo-mechanical and experimental analysis of double pass line heating”, *J. Mar. Sci. Appl.*, **10**, 190-198. <https://doi.org/10.1007/s11804-011-1059-0>
- Clausen, H.B. (2000), Plate Forming by Line Heating. Ph.D Thesis, Technical University, Denmark.
- Das, B. and Biswas, P. (2015), “Effect of operating parameters on plate bending by laser line heating”, *Proceedings of the Institution of Mechanical Engineers, Part B: Journal of Engineering Manufacture*, **231**(10), 1812-1819. <https://doi.org/10.1177/0954405415612678>.
- Iwamura, Y. and Rybicki, E.F. (1973), “A transient elastic-plastic thermal stress analysis of flame forming”, *J. Eng. Ind.*, **95**(1), 163-171. <https://doi.org/doi:10.1115/1.3438093>.
- Lewis, R.W., Morgan, K., Thomas, H.R. and Seetharamu, K.N. (1996), *The Finite Element Method in Heat Transfer Analysis*. 1st ed, Hoboken, NJ: Wiley.
- Moshaiov, A. and Vorus, W.S. (1987), “Mechanics of the flame bending process: Theory and applications”, *J. Ship Res.* **31**(4), 269-281. <https://doi.org/10.5957/jsr.1987.31.4.269>.
- Seong, W.J., Ahn, J., Na, S.J., Han, M.S. and Jeon, Y.C. (2010), “Geometrical approach for flame forming of single curved ship hull plate”, *J. Mater. Process. Technol.*, **210**(13), 1811-1820. <https://doi.org/10.1016/j.jmatprotec.2010.06.013>.
- Srinath, L.S. (2009), *Advanced Mechanics of Solids*. 3rd Ed., Tata McGraw-Hill, USA.
- Thomas, K., Sharma, R. and Bhattacharya, S.K. (2018), “A computer simulation model for thermal forming of ship and offshore structures”, *J. Ship Product. Design*, **34**(4), 279-309. <https://doi.org/10.5957/JSPD.160030>.
- Ueda, Y., Murakawa, H., Rashwan, A.M., Neki, I., Kamichika, R., Ishiyama, M. and Ogawa, J. (1994), “Development of computer-aided process planning system for plate bending by line heating (Report 3)—relation between heating condition and deformation”, *J. Ship Product.*, **10**(4), 248-257. <https://doi.org/10.5957/jsp.1994.10.4.248>.
- Ugural, A.C. (2010). *Stresses in Beams, Plates, and Shells*. 3rd Ed., CRC Press, USA.
- Zhang, L., Reutzel, E.W. and Michaleris, P. (2004), “Finite element modeling discretization requirements for the laser forming process”, *Int. J. Mech. Sci.*, **46**(4), 623-637. <https://doi.org/10.1016/j.ijmecsci.2004.04.001>.